Distribution Category:
Energy Conversion
(UC-93)

ANL-82-40

ANL--82-40

DE82 021272

ARGONNE NATIONAL LABORATORY
9700 South Cass Avenue
Argonne, Illinois 60439

ADVANCED-FUEL-CELL DEVELOPMENT

Progress Report for
April—June 1981

by

R. D. Pierce, R. M. Arons,* J. T. Dusek,* A. V. Fraioli,
G. H. Kucera, J. W. Sim, and J. L. Smith

Chemical Engineering Division

August 1982

Previous reports in this series

ANL-80-98	April—June 1980
ANL-81-16	July—September 1980
ANL-81-67	October—December 1980
ANL-81-68	January—March 1981

*Materials Science Division, ANL.

TABLE OF CONTENTS

LIST OF FIGURES

LIST OF TABLES

ADVANCED FUEL CELL DEVELOPMENT

Progress Report for
April-June 1981

by

R. D. Pierce, R. M. Arons*, J. T. Dusek*, A. V. Fraioli,
G. H. Kucera, J. W. Sim, and J. L. Smith

ABSTRACT

This report describes fuel cell research and development activities at Argonne National Laboratory (ANL) during the period April through June 1981. These efforts have been directed toward (1) improving understanding of component behavior in molten carbonate fuel cells and (2) developing alternative concepts for components.

The principal focus has been on the development of sintered γ-$LiAlO_2$ electrolyte supports, stable NiO cathodes, and hydrogen diffusion barriers. Cell tests were performed to assess diffusion barriers and to study cathode voltage relaxation following current interruption.

SUMMARY

Electrolyte Development--Sintered Electrolyte Support

Sintered γ-$LiAlO_2$ plates can be prepared routinely by sintering tapes prepared from β-$LiAlO_2$ synthesized by the spray-drying procedure. However, efforts to impregnate the sinters have been unsuccessful, because the impregnated bodies contain cracks. We believe the cracking occurs during the salt shrinkage that accompanies freezing and cooling.

Several measures will be examined to avoid the cracking; these include increasing the sinter's strength, nucleating voids in the salt, and using an off-eutectic salt composition.

Electrode Development

Sintered Nickel Oxide Cathodes

Two 150-cm^2 cathodes were prepared by cold-pressing and sintering agglomerates of lithiated nickel oxide. These cathodes were 1.00- and 1.07-mm thick, but the maximum thickness that can be accommodated by the present cell hardware is 0.75 mm. The Argonne Optics Shop attempted to grind these cathodes to the required dimension. One broke into many pieces, but the other was ground to an acceptable thickness, although it was cracked in the process. Cathode cracks are tolerable in a cell, and this cathode can be used

* Materials Science Division (MSD), ANL.

in a cell test. We are attempting to achieve the greater strength necessary to prepare thinner plates by incorporating reinforcing fibers in the green bodies. Lithium, which has been used as a sintering aid in preparing other ceramic materials, is being investigated for its effect on the sintering of NiO.

Experiments are under way to investigate organic fibers as pore formers in sintered cathodes. Two approaches are being followed: (1) introducing pores by burning out short fibers dispersed with the NiO and (2) impregnating a fiber cloth with nickel solution such that the cloth serves as a sacrificial skeleton for the final body.

Plates were prepared by cofabricating an electrolyte structure and a sintered cathode by two processes: (1) sequentially cold-pressing $LiAlO_2$ and NiO as layers in the die and (2) spraying wet NiO onto a green or fired $LiAlO_2$ plate. The composites were fired for 1 to 1.5 h at 1000 to 1030°C. The second approach is attractive if we can show that thin (about 0.02 mm) cathodes are desirable.

It has been noted that there is a wide discrepancy in the NiO density listed in various references. We believe the best value is 6.808 g/cm^3, which is based on X-ray diffraction data by Toussaint.

Nickel Aluminate

Nickel aluminate was prepared by reacting $Ni(NO_3)_2$ and Al_2O_3 for two hours at 1600°C. Some of the product was exposed to 78% H_2-19% CO_2-3% H_2O to reduce a portion of the nickel. A laminated cathode was prepared by spraying a thin layer of the partially reduced $NiAl_2O_4$ onto a standard preoxidized cathode. This cathode was used in cell SQ-25. Posttest evaluation of the results will be performed next quarter.

Cell Testing

Cell Operation

Recent cells, SQ-20 through -25, were assembled with tiles containing high-surface-area γ-$LiAlO_2$ and 64 wt % Li_2CO_3-K_2CO_3 eutectic and with preoxidized cathodes. Wet-seal leakage problems earlier associated with the in situ oxidation of the cathode have been eliminated by the use of preoxidized cathodes. Cell performance has been good, but hydrogen crossover was observed in each cell.

Coatings of fine $LiAlO_2$ applied as a diffusion barrier to the anode surface adjacent to the tile in several cells decreased, but did not eliminate, hydrogen crossover. However, problems were encountered in applying satisfactory coatings, and further work will be done on providing an anode-side diffusion barrier.

Similarly, a layer of fine $NiAl_2O_4$ was applied to the tile side of the cathode for cell SQ-25. Although the posttest examination is incomplete, the results will be clouded by other cell problems, and this test will be repeated.

$LiAlO_2$ Stability/Posttest Evaluation

The $LiAlO_2$ powders from electrolye tiles used in cells SQ-20 through -24 were stable to allotropic transformation throughout the tests, except that a small amount of γ-Al_2O_3 originally present reacted to form $LiAlO_2$. The surface area of the particles decreased by about 1/3 in 1000 h. In all four cells, β-$LiAlO_2$ was used as a diffusion barrier on the anodes. The β-$LiAlO_2$ transformed to α-$LiAlO_2$ in two cells and to γ-$LiAlO_2$ plus some lithium-nickel oxide in the other two, in which only a small amount of β-$LiAlO_2$ was applied.

A carbonate material balance was attempted among the components of these tests. The material balances were not good, indicating the difficulty in getting representative samples of each component. Cathodes contained carbonates equivalent to 32-45% of their void volume. For tests where carbonates were added at assembly at the anode-tile interface, excess carbonates were apparent only in the anode.

Plasma Spraying of Cell Housing

We have begun efforts to use ANL plasma spraying equipment to apply aluminum on the cell housings, which provides the corrosion protection required in the wet-seal region. The aluminum was applied to earlier hardware by flame spraying by an outside vendor who no longer can provide the service.

Potential Relaxation Experiment

A test cell was equipped with four reference electrodes in the cathode gas and one in the wet-seal area. The cell performance is not up to our state of the art, but it is adequate enough to permit meaningful potential-relaxation data to be obtained. The potential of the internal reference electrodes relaxes more rapidly than that of the reference electrode in the wet-seal area.

I. INTRODUCTION

The advanced fuel cell studies at Argonne National Laboratory (ANL) are part of the DOE Advanced Fuel Cell Program. The objective of this DOE program is to reduce the technical uncertainties with fuel cells so that manufacturers and users can introduce high-efficiency generating systems that have the capability of operating on coal or other fuels. At the present stage of development, the primary thrust of the ANL program is to provide supporting research and development that pursues fundamental understanding of fuel cell behavior and investigates alternative stack concepts.

A molten carbonate fuel cell consists of a porous nickel anode, a porous lithiated nickel oxide cathode, an electrolyte structure which separates the anode and cathode and conducts only ionic current between them, and appropriate metal housings or, in the case of stacks of cells, intercell separator sheets. The cell housings (or separator sheets) bear upon the electrolyte structure to form a seal between the environment and the anode and cathode gas compartments. The usual electrolyte structure, which is commonly called "tile," is a composite of discrete $LiAlO_2$ particles and a mixture of alkali metal carbonates. The carbonates are liquid at the cell operating temperature of 925 K. At the anode, hydrogen and carbon monoxide in the fuel gas react with carbonate ion from the electrolyte to form water and carbon dioxide while giving up electrons to the external circuit. At the cathode, carbon dioxide and oxygen react and accept electrons from the external circuit to re-form carbonate ion, which is conducted through the electrolyte to the anode. In a practical cell stack, CO_2 for the cathode probably would be obtained from the anode exhaust.

The ANL contribution to the program is intended to provide understanding of cell behavior and to develop improved components and processes. The electrolyte structure and cathode are receiving special study at ANL. Electrolyte structures employing a sintered $LiAlO_2$ matrix are being examined as an alternative to tiles, which are a paste-like mixture of fine $LiAlO_2$ particles and carbonate salt. Characterization of electrolyte-structure properties and the relation of these properties to cell behavior are of major importance. Determination of the stability of the structure is also of high priority.

Current practice involves assembling molten carbonate fuel cells with a sintered nickel cathode, which reacts *in situ* with the oxidant gas and the electrolyte to form lithiated nickel oxide. The lithiation is important in that it gives the cathode adequate electronic conductivity. ANL is investigating preparation of nickel oxide cathodes for assembly in cells. This is expected to improve cell performance through better conductivity, strength, and dimensional stability of the cathode. Lithiation may be performed in cell or out of cell.

Cells are operated to assess the behavior of the electrolyte and other components and to understand the performance and life-limiting mechanisms at work within the cell. Cell operation is coupled with an emphasis on diagnostics and materials development.

II. ELECTROLYTE DEVELOPMENT--SINTERED ELECTROLYTE SUPPORT
(J. W. Sim)

We are developing sintered $LiAlO_2$ electrolyte retainers, using tape casting to produce the green body for subsequent sintering. In the last quarterly (ANL-81-68, p. 7), we reported that crack-free tapes were produced routinely and that sintering of the tapes was straightforward, but that impregnation of the porous sinters with molten carbonates was a problem. It appeared from our preliminary experiments last quarter that cracking during impregnation was due either to (1) differential thermal contraction between the impregnated sinter and the support plate on which it rested and to which it adhered, or (2) incomplete filling of the pores of the sintered body. During this quarter, steps were taken to minimize adhesion of the impregnated sinters to their support and to determine whether the level of filling of the pores with carbonates affected the cracking that occurred during impregnation. To date, carbonate impregnation has caused cracking of all sintered structures prepared from tape-cast green bodies. We now suspect that cracking is caused by the large change in volume of the carbonates during cooling from 600°C to room temperature. Our present emphasis is on developing methods that accommodate the volumetric change without cracking.

The slip formulation experiments performed during this quarter are given in Table 1. Casting was performed by the technique discussed earlier (ANL-81-68, p. 7), and few problems were encountered in obtaining satisfactory tapes. Occasionally, a skin formed on the surface of the slip during casting, and this caused the dry tape to have a rough surface. Sintering of the tapes was straightforward, and the porosities obtained are summarized in Table 2. In the early sintering experiments, porous alumina cover plates contacted both faces of the tape. After several uses, the cover plates acquired a residue that caused some tapes to crack during sintering. In our recent sintering experiments, high-density alumina plates were used, and the top cover plate was suspended above the tapes by spacers (about 5 mm). Flat, crack-free sinters were obtained consistently by the more recent technique.

Table 1. Summary of Slip Formulation Experiments

	Weight, g					
	$LiAlO_2$	PX316[a] Plasticizer	UCON[b] Plasticizer	B-98[c] Binder	Solvent[d]	Viscosity, cps
SN-216-61	145	15	16	21	178	3700
SN-216-67	80	11	12	12	105	2425
SN-216-87	189	22	23	17	209	--
SN-216-105	231	25	32	46	329	1440

[a]Mixed normal alkyl phthalates, USS Chemicals product PX316.
[b]Polyethylene glycol, Union Carbide product UCON 50-HB-2000.
[c]Polyvinyl butyral, Monstanto product Butvar B-98.
[d]40 wt % ethanol, 60 wt % xylene.

Table 2. Summary of Sintering Experiments

Sinter No.	Sintering Temperature, °C	Sintering Time, h	Porosity, %
S-216-110-1	1000	2	73
S-216-110-3	1000	2	73
S-216-112-2[a]	1000	1	--
S-216-115-1	1050	3	71
S-216-115-2	1050	3	70
S-216-115-3	1050	3	70
S-216-115-4	1050	3	71
S-216-116-1	1050	1	71
S-216-116-2	1050	1	71
S-216-116-3	1050	1	72
S-216-116-9[a]	1120	1	--
S-216-116-10	1120	1	65
S-216-117-1	1120	1	65
S-216-117-2	1120	1	65
S-216-117-3	1120	1	66
S-216-117-4	1120	1	66
S-216-118-1	1175	1	61
S-216-118-2	1175	1	61
S-216-118-3[a]	1175	1	--
S-216-118-4	1175	1	62
S-216-118-5	1175	1	62
S-216-71-1	1000	2	72
S-216-72-2	1000	2	73
S-216-72-3	1000	2	72
S-216-7-4	1000	2	71
S-216-76-2	1050	3	68
S-216-76-4	1050	3	66
S-216-76-1	1050	3	66
S-216-96-1	1050	2	71
S-216-96-2	1050	2	71

[a]X-ray diffraction analysis by B. S. Tani (Analytical Chemistry Laboratory, ANL) indicates γ-$LiAlO_2$ as a major phase and $LiAl_5O_8$ as a very minor phase.

In general, the handling strength of the tapes improved with sintering temperature; however, even the samples sintered at 1000°C (about 70% porosity) had sufficient strength to allow the handling necessary to measure their dimensions.

Prior to carbonate impregnation, each of the sinters was examined for cracks. This examination was accomplished by illuminating the sample from behind with a high intensity lamp and looking for transmitted light. None of the sinters used for impregnation experiments showed signs of cracks by this examination. In future experiments, we plan to examine the sinters for cracks by X-ray radiography prior to impregnation. The impregnation procedure involved covering the surface of the sinter with Li_2CO_3-K_2CO_3 (62-38 mol %) eutectic and then infusing the carbonates by heating the sinter to 600°C. To avoid thermal shock to the sinters, the cooling rate was maintained at about 100°C/h. To minimize adhesion, a Kanthal* screen was placed between the sinter and the alumina plate on which it was resting. The percentage of pores filled by the carbonates was changed by varying the quantity of eutectic placed on top of the sinter. The results of the impregnation experiments performed during this quarter are given in Table 3.

All of the impregnated sinters cracked during impregnation, but some of them had only very small cracks (about 0.02 by 5 mm). None of the sinters adhered to the alumina plate, but some adhered slightly to the Kanthal screen.

Table 3. Summary of Impregnation Experiments

Impregnation Number	Sinter Number	Porosity, %	Sintering Conditions	Eutectic Filling[a]
I-216-79-1	S-216-71-1	72	2 h at 1000°C	90%
I-216-80-2	S-216-72-2	73	2 h at 1000°C	95%
I-216-81-3	S-216-72-3	72	2 h at 1000°C	100%
I-216-82-4	S-216-73-4	71	2 h at 1000°C	110%
I-216-85-2	S-216-76-2	68	3 h at 1050°C	95%
I-216-86-4	S-216-76-4	66	3 h at 1050°C	100%
I-216-84-1	S-216-76-1	66	3 h at 1050°C	90%
I-216-101-1	S-216-96-1	71	2 h at 1050°C	100%
I-216-101-2	S-216-96-2	71	2 h at 1050°C	100%

[a]Ratio of volume carbonate eutectic charged to porosity; assumes carbonate density of 1.94 g/cm^3.

*Type A1, Kanthal Corp., Bethel, CT.

It is doubtful that such light adhesion was sufficient to cause cracking. However, it would appear that the level of pore filling (in the range examined) has no effect on cracking, as all of the sinters cracked during impregnation.

We suspect that cracking during impregnation results from the large decrease in volume that occurs in the carbonate phase during cooling from 600°C to room temperature. (This volume reduction increases the density from 1.96 to 2.27 g/cm^3.) A 9% volumetric change occurs during freezing. This volumetric change, as well as that occurring after freezing, requires one of the following processes to occur: (1) a decrease in the total volume of the impregnated structure or (2) formation of voids within the impregnated structure. The former process cannot occur by rearrangement of particles because the $LiAlO_2$ particles are bonded by sintering. The latter process can occur only if the sintered body is sufficiently strong to withstand the stresses generated by the contracting carbonates; otherwise cracks will form and propagate to relieve the stress. This analysis is consistent with the observation that porous metal anodes of similar porosity and geometry but greater strength can be filled with carbonates without cracking.

We plan to examine several measures that may alleviate the cracking problem, including (1) increasing the strength of the porous sintered $LiAlO_2$ structures, (2) nucleating voids in the carbonate phase that can accommodate contraction without generating sufficient stress to crack the structure, and (3) using off-eutectic carbonate compositions so that freezing of the electrolyte (and the associated stress) occurs over a range of temperatures. Some of the sintered structures in Table 2 were sintered at high temperatures to increase their strength. However, whether the high temperatures will increase their strength sufficiently is uncertain since there is a practical limit to the level of sintering that is acceptable. At high sintering temperatures, fine porosity disappears and γ-$LiAlO_2$ decomposes to $LiAl_5O_8$. Since voids might be introduced by release of gases that are dissolved in the carbonates, impregnation experiments will be performed with several different gas atmospheres.

III. ELECTRODE DEVELOPMENT

The reference procedure for preparing cathodes for molten carbonate fuel cells has been to oxidize and lithiate a porous nickel plaque in the cell after startup. This in situ oxidation is accompanied by expansion of the electrode and fragmentation of the nickel into small crystallites of lithiated nickel oxide. In the oxidized structure, the fine pores between the crystallites retain electrolyte for ion conduction, and the coarse pores originally present in the nickel promote gas movement. The crystallite formation also increases reaction surface. However, the expansion of the electrode causes sealing problems, and the fragmentation weakens the structure and increases electrode resistance. Also, the in situ oxidation does not allow much control of the cathode microstructure. Therefore, we are attempting to develop cathodes that are structurally stable and have a tailored microstructure.

A. Sintered Nickel Oxide Cathodes
(R. M. Arons and J. T. Dusek)

1. Cold Pressing and Sintering

Two cathodes (nominally 150 cm^2) have been prepared using agglomerates of -200 +270 and -270 +325 mesh. After cold-pressing and sintering, they were 1.00- and 1.07-mm thick, respectively. Because the test cells can only accommodate a maximum 0.75-mm thick cathode and also because some machinability of cathodes may be desirable, we decided to evaluate whether the cathodes could be ground to the required thinness by the ANL Central Shops. One of the plates was too weak to grind without introducing numerous fractures. The other plate was ground, with only one major fracture and some minor cracking along one edge. This cathode can be used for cell testing.

The limiting factor regarding cold-pressing and sintering cathode plates as thin as required is the low strength of the green body, which prevents successful removal of a <0.75-mm thick plate from the cold-press die. We have pressed a 0.65-mm thick cathode onto a substrate (see below). Currently, we are attempting to provide the required strength by reinforcing the green bodies with fibers. The results of this work will be presented in future reports.

Lithium is often used as a sintering aid in ceramic materials such as MgO and Al_2O_3. The defect structure induced by introducing a small monovalent ion into NiO suggests that lithium also will enhance sintering in NiO. The effect of lithium as a sintering aid in NiO was investigated in a series of disk-shaped NiO specimens that all had been prepared in the same manner, except that varying amounts of Li_2CO_3 dopants were used. Preliminary analyses of these disks indicated that 2-1/2% lithium addition enhanced sintering and 5 to 10% lithium had little effect.

2. Use of Pore Formers

To obtain more large pores in cathodes, we have begun experiments using both natural and synthetic organic fibers as pore formers. These fibers, when incorporated into a green NiO body, will burn out during firing and leave

voids or pore channels in the sintered bodies. We currently are pursuing two approaches. In the first, short chopped fibers are dispersed in a body and burned out. The problem associated with this approach is that it is difficult to obtain homogeneous dispersal of fibers and a high enough volume fraction of fiber in the body. The second approach involves coating woven cloth or organic fibers with NiO so that the cloth serves as a sacrificial skeleton for the final body.

We have demonstrated that the fibers can be successfully burned out during firing by either approach. For fibers dispersed in an NiO body, the fibers leave pore channels behind upon burning. For the coated-cloth approach, if a nickel salt such as $NiCl_2$ is dissolved in the liquid used to suspend the NiO powder, it will permeate the fibers and convert to NiO during firing. This NiO has been observed by scanning electron microscopy (SEM) to create a NiO replica of the original fiber. This appears to be a reasonable way of creating fibrous NiO structures, although the fibers have low strength.

3. Cofabrication of Sintered Cathode and Electrolyte Structures

We are pursuing two potential methods for fabricating a monolithic cathode/electrolyte structure. One means is by spraying wet, lithiated NiO agglomerates onto either a green or fired $LiAlO_2$ plate (cold-pressed). The second method is cold-pressing a layer of NiO agglomerates onto a cold-pressed $LiAlO_2$ plate. In either case, the composite is fired for 1-1.5 h at 1000-1030°C.

Presently, there is considerable uncertainty regarding the optimum cathode thickness. One opinion is that the cathode must be of the order of 0.7-mm thick so that sufficient catalytic surface is provided for it to function properly; another opinion is that only a "shadow of a cathode" is required, perhaps <0.05 mm. Spraying can produce a cathode as thin as 0.02 mm, whereas cold-pressing can produce a 0.7-mm cathode.

A few composite plates were produced by spraying calcined agglomerates. An example of the structure developed is shown in Fig. 1. The NiO layer is roughly 0.03 mm or one agglomerate diameter thick. The fine pore structure within the agglomerates has been retained, but the identity of individual agglomerates has been lost. This agglomerate loss may be due to (1) impact damage to the agglomerates upon striking the $LiAlO_2$ substrate, (2) fracture of the agglomerates when traversing the sprayer, or (3) selective suspension of fine agglomerates in the sprayed slip. The loss of agglomerate integrity is not necessarily bad for cathode performance, however, because the gas diffusion distances through such a thin cathode are not large. We are investigating means to retain the agglomerate shape should it prove to be useful.

An example of a composite structure formed by cold-pressing a lithiated-NiO agglomerate layer on a $LiAlO_2$ substrate is shown in Fig. 2. The original NiO agglomerates were compounded by mixing reagent grade NiO and Li_2CO_3 powders with 6 wt % polyvinyl alcohol (PVA) in water, drying, crushing, and screening to -200 +270 mesh. The $LiAlO_2$ substrate was similarly made by crushing and screening 3 wt % PVA to -200 mesh. The $LiAlO_2$ was added to the die and troweled to a smooth flat layer; the NiO was then added on top of the

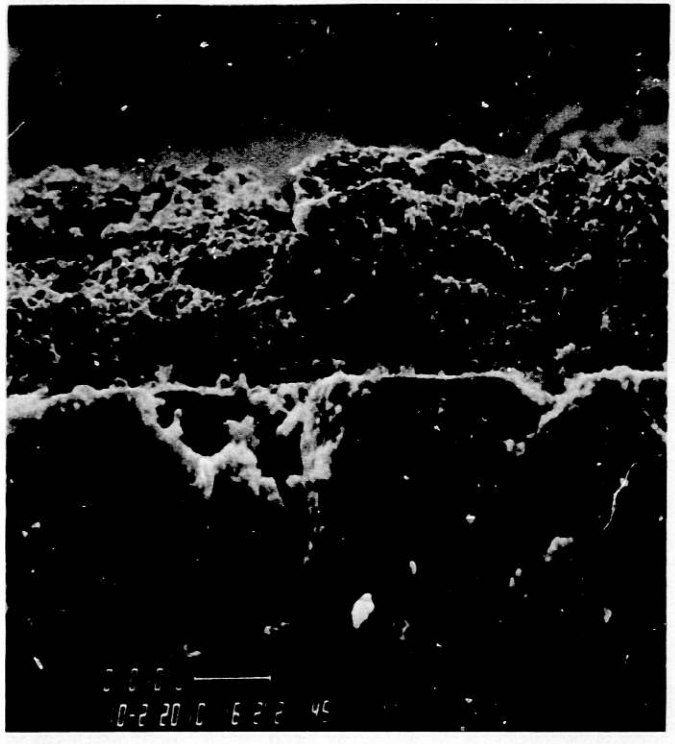

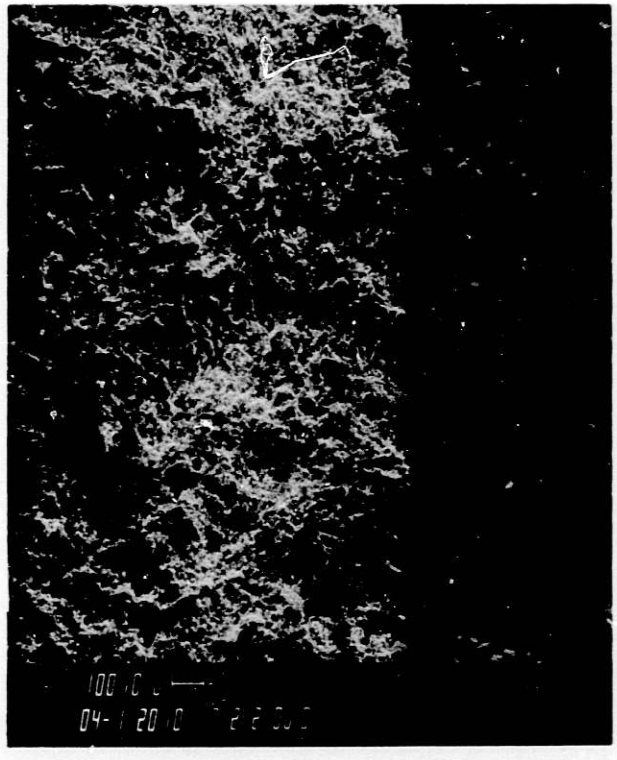

ANL Neg. No. 306-81-140.

Fig. 1. Lithiated NiO Cathode Layer on $LiAlO_2$ Substrate Applied by Wet Spraying and Firing. Scale marker is 10 μm.

Fig. 2. Lithiated NiO Cathode Layer (right) on $LiAlO_2$ Substrate (left) Applied by Cold Pressing and Firing. Scale marker is 100 μm.

$LiAlO_2$ and troweled flat. The top punch was then put in position, and the composite was pressed at 14 MPa (2000 psi) and fired for 1 h at 1000°C. The flatness of the NiO layer, the good contact at the interface, and the integrity of the NiO agglomerates are apparent in Fig. 2. The NiO layer is 0.6-mm thick, while the $LiAlO_2$ is 1.2-mm thick.

4. Nickel Oxide Density

We have noted that NiO density data reported in the 1960 Handbook of Chemistry and Physics[1] are in error. This reference and others of similar vintage list the density of NiO as 7.45 g/cm^3. The currently accepted value based on the X-ray diffraction work of Toussaint[2] is 6.808 g/cm^3. From Fig. 3 of Toussaint, one may generate an expression for the theoretical or X-ray density (TD) of NiO containing a given cation percent lithium as:

$$TD = \frac{(\text{molecular weight})(4)}{(\text{unit cell volume})(6.023 \times 10^{23})}$$

where molecular weight = 74.7 (1 - x) + 22.9(x) and unit cell volume = -9.327(x) + 72.88.

B. Nickel Aluminate
(A. V. Fraioli)

As mentioned in the last report (ANL-81-68, p. 14), a 1/2 kg batch of $NiAl_2O_4$ was prepared by fusion of γ-Al_2O_3 and $Ni(NO_3)_2$ for two hours at 1600°C. Approximately thirty grams were transferred to a motor-driven mortar and pestle and ground for a period of two hours. Two 5-g aliquots of the fine powder, along with two 5-g aliquots of unground powder, were transferred to four alumina cups and reduced in 78% H_2-19% CO_2-3% H_2O at 650°C. The first two cups (one of coarse and one of fine aluminates) were removed from the furnace after 25 h; the last two cups were withdrawn after 97 h.

X-ray diffraction (XRD) analysis* showed almost no difference among the samples; the expected major lines of $NiAl_2O_4$ spinel (>50%), minor nickel (10-30%), and very minor NiO (3-10%) were found. The powders were further characterized by SEM photomicrographs and BET surface area measurements,* the results of which are summarized in Table 4. The original gray-green nickel aluminate darkened after the 25-h reduction; the 97-h samples were jet-black. The photomicrophotographs showed the unground material to be composed of large chunks, in the 30-50 μm range, with a small distribution of 1-μm fines, while the ground samples were shown to be composed primarily of submicron particles, with a few chunks in the 30-50 μm range. The 97-h aluminates, both ground and unground, had higher surface areas than the 26-h ones.

A 50 wt % suspension of sample NB 202-107-2 was ball-milled in 1% aqueous ammonium alginate for 8 h and then further diluted in an equal volume of distilled water to a suitable spraying consistency. Trial spraying showed that

*Throughout this report, B. S. Tani performed XRD analysis and R. Malewicki performed BET measurements. Both analysts are members of ANL's Analytical Chemistry Laboratory.

Table 4. Characterization of Nickel Aluminate

Sample	Preparation	SEM Particle Size	Color	BET Surface Area, m^2/g
NB 202-105-2	1 kg prep	>100 μm	gray-green	1.9
NB 202-107-1[a]	reduced 26 h, 650°C	submicron fines, some 30-50 μm	dark green	0.35
NB 202-107-2[a]	reduced 97 h, 650°C	submicron fines, some 30-50 μm	jet black	4.9
NB 202-107-3[b]	reduced 26 h, 650°C	1 μm, with 30-50 μm chunks	dark green	0.72
NB 202-107-4[b]	reduced 97 h, 650°C	1 μm, with 30-50 μm chunks	jet black	2.41

[a]Ground for 2 h with mortar and pestle.

[b]As-prepared in 1 kg batch.

smooth, coherent surface coats could be applied to preoxidized cathode surfaces, with penetration extending no farther than the surface macropores (10-15 μm); consequently, a layer of $Ni/NiAl_2O_4$ containing reduced nickel was spray-coated onto a preoxidized NiO cathode and prepared for incorporation in test cell SQ-25. The test results, described elsewhere in this report, were inconclusive because the anode wet-seal failed.

IV. CELL TESTING

A. Cell Operation

(J. L. Smith, J. W. Sim, J. R. Stapay, and A. V. Fraioli)

In recent tests, 94-cm^2 cells (SQ-20 through SQ-25) were assembled with high-surface-area (~30 m^2/g) γ-$LiAlO_2$ tiles containing 64 wt % eutectic and with preoxidized cathodes. A description of cells SQ-20 to SQ-25 is presented in Table 5. In these cells, the cathode expansion problem, observed with all *in situ* oxidized cathodes, has been eliminated by the use of preoxidized cathodes. Moreover, the previously reported problem of hydrogen crossover from the anode to cathode gas stream has been reduced, but not eliminated, by use of barriers.

Cells SQ-21 and SQ-22 had barriers of fine (about 0.2 μm) β-$LiAlO_2$ particles sprayed on the anode surface, and both had eutectic added at the anode/tile interface during cell assembly. In both cases, hydrogen crossover was less than that of cell SQ-20, but both cells had abnormally high resistance (9-14 mohm). Posttest examination revealed that surface roughness of the $LiAlO_2$ layer resulted in poor contact with the tile and caused the high resistance.

Table 5. Summary of Cells SQ-20 through -25

	SQ-20	SQ-21	SQ-22	SQ-23	SQ-24	SQ-25
Preoxidized Cathode Thickness, mm	0.51	0.38	0.38	0.38	0.38	0.38
NiCr Anode Thickness, mm	0.76	0.76	0.76	0.76	0.76	0.76
Tile	← 64 wt % eutectic with ~30 m^2/g γ-$LiAlO_2$ →					
Barrier	None	$LiAlO_2$ on anode	$LiAlO_2$ on anode	$LiAlO_2$ in anode surface	Same	$NiAl_2O_4$ on cathode
Added Eutectic, g	None	2.4	1.2	None	1.2	1.2
Test Duration, h	460	438	293	459	342	196
Resistance, mohm	6.5	9	14	6.6	9	8

Cell SQ-23 incorporated a barrier of β-$LiAlO_2$ in the surface pores of the anode at the tile interface, but did not have electrolyte added during cell assembly. The resistance of SQ-23 was 6.6 mohm, or about the same as that of SQ-20. This thinner diffusion barrier was less effective in stopping hydrogen crossover than were the barriers of SQ-21 and SQ-22.

Cell SQ-24 was identical to SQ-23, except that 1.2 g of electrolyte was added at the tile/anode interface. This cell went through two inadvertent thermal cycles at approximately 80 and 283 h. The cell had cross leakage resulting in 4.4×10^{-4} mol/min of water in the cathode exhaust, which is comparable to the leakage in cell SQ-20. The leakage reduced slightly after the second thermal cycle. The cause of the high resistance (9 mohm) of cell SQ-24 is not known with certainty; all components separated easily at post-test disassembly. This high resistance may have resulted from the cumulative effect of several poor interfacial contacts.

Cell SQ-25 was similar to SQ-24, except that the diffusion barrier was a layer of nickel aluminate with ammonium alginate binder sprayed on the tile side of the cathode rather than $LiAlO_2$ applied to the anode. This cell had severe anode wet-seal leakage (about 70% wet-seal efficiency) throughout operation; the cathode wet-seal efficiency was always greater than 95%. The amount of water in the cathode exhaust was comparable to other cells that had a diffusion barrier. The current-voltage performance also was similar to that of recent cells. Cell disassembly revealed two anomalies that could affect wet-seal efficiency. First, the current collector was shifted from its intended position, which could have resulted in the anode not being recessed from the wet-seal as intended. Second, the insulation had contacted the tile in one area and had wicked carbonates from the tile.

In summary, performance* has been good (0.72 V at a current density of 160 mA/cm^2) and quite reproducible for all cells except SQ-21 and SQ-22, which had diffusion barriers with rough surfaces. Variations in wet-seal efficiency and in cross leakage have not caused large variations in performance. The earlier problems of cathode expansion and performance nonreproducibility seem to have been eliminated by the use of preoxidized cathodes. Work will continue on development of a diffusion/bubble barrier to block the persistent problem of hydrogen crossing over from the anode to the cathode.

B. $LiAlO_2$ Stability/Posttest Evaluation
(G. H. Kucera)

During the past quarter, the posttest components from cells SQ-20 through -24 were examined (1) to determine the stability of $LiAlO_2$ in the electrolyte tiles as well as in the hydrogen diffusion barriers at the anode-tile interface and (2) to determine the carbonate content of each of the components. In addition, aqueous solutions of the carbonates removed from specimens of the cell components from cells SQ-20, -21, and -22 were analyzed for metals having

*Utilization: Fuel, 75%; oxidant, 25%.
Fuel: 77.6% H_2-19.4% CO_2-3%H_2O.
Oxidant: 28% CO_2-14.5% O_2-57.5% N_2.

atomic numbers of 19 (potassium) or greater by the dispersive X-ray fluorescence technique. The $LiAlO_2$ powders were washed free of carbonates by an acetic acid-acetic anhydride mixture and characterized by X-ray diffraction analysis and BET surface area measurements; the diffusion barriers were examined by scanning electron microscopy (SEM). The carbonate content for a portion of a component was determined by relating the area and/or weight of the portion to that of the whole.

The X-ray diffraction analyses of the $LiAlO_2$ powders contained in the electrolyte tiles in cells SQ-20 through -24 show little or no phase changes. Both before and after cell testing, γ-$LiAlO_2$ was present as a major phase, β-$LiAlO_2$ as a medium phase, and α-$LiAlO_2$ as a minor to very minor phase. The only exception was that unreacted γ-Al_2O_3 in the initial electrolyte mixtures reacted during cell operation to form $LiAlO_2$. For cells SQ-21 to -24, the $LiAlO_2$ powder used in the hydrogen diffusion barriers, formed by placing a β-$LiAlO_2$ layer on the anode at the anode/tile interface, consisted of β-$LiAlO_2$ as a major phase and α-$LiAlO_2$ as a possible, very minor phase. Table 6 is a summary of the phase composition of the $LiAlO_2$ from the diffusion barriers of cells SQ-21 through -24.

Table 6. Stability of $LiAlO_2$ Used as a Hydrogen Diffusion Barrier in Test Cells SQ-21 through -24

Cell Number	Initial Condition of Barrier	Posttest Phase(s)	
Initial Powder	---	β-$LiAlO_2$	major
		α-$LiAlO_2$	very minor, possible
SQ-21 (438 h)	on anode, rough surface	α-$LiAlO_2$	major
		Ni	minor
		β-$LiAlO_2$	minor
		γ-$LiAlO_2$	minor
SQ-22 (293 h)	on anode, rough surface	α-$LiAlO_2$	major
		β-$LiAlO_2$	major
		Ni	minor
SQ-23 (459 h)	in anode surface pores	γ-$LiAlO_2$	major
		β-$LiAlO_2$	medium
		Li-Ni oxide	medium
		Ni	minor
SQ-24 (342 h)	in anode surface pores	Li-Ni oxide	major
		γ-$LiAlO_2$	medium
		β-$LiAlO_2$	medium

The data show that the β-$LiAlO_2$ in SQ-21 and -22 transformed primarily to the α- phase, whereas the β-$LiAlO_2$ in SQ-23 and -24 transformed to γ-$LiAlO_2$ and also a hexagonal lithium nickel oxide. Samples of $LiAlO_2$ taken from the tile adjacent to the diffusion barrier/tile interface do not show similar transformations; the composition of that $LiAlO_2$ remained unchanged.

Table 7 presents surface area data for the $LiAlO_2$ powder from electrolyte tiles for cells SQ-20 to -24. The data show a $LiAlO_2$ surface area loss of about 25% after 500 h; an earlier cell (SQ-17) showed a $LiAlO_2$ surface area loss of about 32% after 1000 h. From these data we conclude that the $LiAlO_2$ will have a surface area loss of about 50% (to about 15 m^2/g) after 40,000 h (the anticipated cell life). Our previous studies[3] reported that $LiAlO_2$ particles with a surface area of about 13 m^2/g are capable of retaining about 60-62 wt % carbonates without deforming excessively (<25%). The current electrolyte tiles contain 64 wt % carbonates at cell assembly, but lose electrolyte to the porous electrodes during initial operation, resulting in a carbonate content of about 60-61 wt %. Thus, little or no tile deformation is expected to accompany this projected surface area loss.

Table 7. Surface Area of $LiAlO_2$ in Tiles

Cell No.	Surface Area, m^2/g		Test Duration, h
	Pretest	Posttest	
SQ-17[a]	35	21	1077
SQ-20	33	21	460
SQ-21	29	27	438
SQ-22	28	28	293
SQ-23	29	19	459
SQ-24	33	20	342

[a]Reported in ANL-80-98, p. 19.

Because of the small quantity of $LiAlO_2$ (0.08 to 0.5 g) used as the hydrogen diffusion barrier, it was not possible to obtain a BET measurement of its surface area. However, samples of the barriers were examined microscopically (SEM). The micrographs show particles about 0.5 μm in size. In general, they appear to be unchanged as a result of cell exposure.

The carbonate content of the anode, cathode, and tile after cell operation was determined for cells SQ-20 through -24; the data are summarized in Table 8. The data show several trends: (1) the addition of carbonates to the anode/tile interface in cells SQ-21, -22, and -24 resulted in a wetter anode, (2) the cathode wetting ranged between 32 and 45% of the void volume and appeared to be unaffected by the wetter anodes, and (3) the agreement between the measured amounts of carbonates lost from the tile and the amounts found in the other components was poor in cells SQ-22 and -23 but better in cells SQ-20, -21, and -24 (≥80%). The lack of correlation between these amounts shows the importance of selecting a representative sample of a given component. In the present study, it was assumed that a single specimen consisting of 15 to 20% of a component was representative of the whole; in future measurements, specimens will be taken from several areas of the cell.

Table 8. Carbonate Content of Posttest Cell Components

Cell No.	Carbonate Content, g				Vol. Carbonates/ Void Vol.	
	Anode	Cathode	Lost from Tile	Total in all Components Excluding Salt Added to Anode	Anode	Cathode
SQ-20	3.2	1.9	4.4	5.5	0.36	0.41
SQ-21	4.7[a]	1.2	4.6	4.0	0.53	0.34
SQ-22	4.5[b]	1.2	2.7	4.8	0.50	0.32
SQ-23	3.7[c]	1.6	3.7[d]	5.5	0.41	0.44
SQ-24	5.3[b]	1.6	5.5	5.8	0.59	0.45

[a]Includes 2.4 g carbonates inserted between tile and anode before cell operation.

[b]Includes 1.2 g carbonates inserted between tile and anode before cell operation.

[c]Average of two separate measurements, 3.9 and 3.5 g.

[d]Two separate but identical measurements.

Aqueous solutions of the carbonates and other water soluble species were dissolved from specimens of the anode, cathode, their respective current collectors, and the tile, and then analyzed by the dispersive x-ray fluorescence technique.* Table 9 is a summary of the water soluble metallic species found in the leached salt from each cell component. The data show (1) the unexplained presence of calcium in the extract from the anode and cathode current collectors in all three cells and (2) the presence of manganese in the salt from the cathode current collector and/or cathode and tile in SQ-21 and -22. The presence of manganese at the cathode surface of the tile was reported in a previous quarterly (ANL-81-68, p. 20). The significance of the location of any of the metallic species found has not yet been established.

Samples of the water soluble species have been prepared from specimens of the components of cells SQ-23 and -24 and will be analyzed in the same manner as the previous ones.

C. Plasma Spraying of Cell Housing

(R. M. Arons,† J. J. Picciolo,† and J. L. Smith)

Electrochemical corrosion of the wet-seal region in the stainless steel cell housing was addressed by Swaroop et al.[4] who had the housings flame-sprayed with aluminum by an outside vendor. The housings were then heat-treated

*Analysis performed by E. T. Kucera, Analytical Chemistry Laboratory, ANL.

†Materials Science Division, ANL.

Table 9. Water Soluble Metallic Species Found in Cell Components

	K	Cr	Fe	Ni	Mn	Ca
SQ-20						
cathode current collector	--	--	--	minor	--	major
cathode	major	--	--	--	--	--
tile	major	--	--	--	--	--
anode	major	minor	very minor	minor	--	--
anode current collector	--	--	medium	--	--	major
SQ-21						
cathode current collector	medium	medium	--	major	minor	major
cathode	major	--	--	--	very minor	medium
tile	major	--	--	--	minor	--
anode	major	--	--	--	--	--
anode current collector	--	major	major	--	--	major
SQ-22						
cathode current collector	--	medium	--	--	--	major
cathode	major	--	--	--	minor	medium
tile	major	--	--	--	very minor	--
anode	major	--	very minor	very minor	--	--
anode current collector	--	--	--	--	--	major

for about 30 min at 1275 K in an inert environment. This heat treatment produces a "diffused layer," which was surmised to be $(FeNiCr)Al_2$. In oxidizing conditions, as occur in the cell, protective Al_2O_3 and $LiAlO_2$ form at the surface.

The vendor that originally provided these coatings has since left the plasma spray business. Since a plasma spray torch is available in MSD, we have begun experimenting to see if we can apply a similar coating in-house. We have successfully sprayed aluminum onto Type 316 stainless steel, but have not been able to spray a continuous coating as thin as the approximate 50-70 μm quoted by Swaroop et al.[1] Heat treating of our experimental coating will be attempted soon.

D. Potential Relaxation Experiment
(L. J. Ryan*)

A fuel cell, LR-2, was started on May 28, 1981. Data obtained from this cell will be used to develop a mathematical model that allows prediction of the potential relaxation in a porous electrode in which both mass transfer and kinetic resistance are present. The 94-cm^2 cell contains five reference electrodes on the cathode side. One electrode is in the wet-seal area and is supplied with a constant gas of oxygen and carbon dioxide. The other electrodes

*PhD thesis student on cooperative thesis program with Illinois Institute of Technology.

are inserted through the current collector and holes in the cathode at selected locations; these electrodes are in the cell cathode gas. All the electrodes employ a gold wire that contacts the electrolyte tile. These reference electrodes permit determination of the cathode overpotential relaxation, from which insight can be gained into cathode performance.

The anode wet-seal efficiency for cell LR-2 is only 85%, but the cathode seal is good. The cell open-circuit voltage is low (1.079 V rather than the anticipated 1.085 V), suggesting some gas cross leakage.

Potential relaxation tests are being performed on this cell. At low cathode gas flow (<200 cm^3/min), the potential of the internal reference electrodes differ by as much as 40 mV. At higher cathode gas flow (200-300 cm^3/min) or rich oxidant (33% O_2-67% CO_2), the potential differences between electrodes are negligible. When no gas is flowing to the wet-seal electrode, the wet-seal reference electrode is at about the same potential as that of the other reference electrodes at the gas outlet. These observations seem consistent with hydrogen diffusion to the cathode electrolyte interface. Because the internal reference electrodes measure the difference between the gold wire in its local environment and the cathode housing, a reduction of oxygen at the interface by reaction with hydrogen would result in a potential difference. At higher cathode gas flow, the plane of hydrogen-oxygen reaction is moved into the tile. Then, the potential difference would be approximately zero.

At 200 to 300 cm^3/min cathode gas flow, the potential of the wet-seal reference electrode was found to relax 95% in about 20 s. The potential of the internal reference electrodes was found to relax more quickly in the first 100 ms and then slowly. Equilibrium was reached in about 100 s for the wet-seal reference electrodes and 10 to 20 s for the internal reference electrodes.

In Cell LR-2, gas switching experiments between standard oxidant (30% CO_2-70% air) and rich oxidant were carried out. The influence of the switching valve's operation was determined by alternating between the same gas, i.e., standard to standard. The result was no change in output, verifying that the valve operation caused no pertubation in cell potential. Thus, rapid switching of gas concentration in the cell is a viable method and will be used to measure diffusion characteristics in porous electrodes.

REFERENCES

1. Handbook of Chemistry and Physics, 42 Edition, C. D. Hodgman, Ed., Chemical Rubber Publishing Co., Cleveland, OH (1960).

2. C. J. Toussaint, J. Appl. Cryst. 4, 292 (1971).

3. K. Kinoshita and G. Kucera, Analysis of the Compressive Strength of $LiAlO_2$/Molten Carbonate Structures, accepted for publication in J. Electrochem. Soc.

4. R. B. Swaroop, J. W. Sim, and K. Kinoshita, J. Electrochem. Soc. 125(11), 1799-1800 (November 1978).